Calhoun: The NPS Institutional Archive

DSpace Repository

Theses and Dissertations 1. Thesis and Dissertation Collection, all items

1972-06

Construction of a carbon dioxide TEA laser

Barr, Douglas Harmon

Monterey, California. Naval Postgraduate School

http://hdl.handle.net/10945/16051

Downloaded from NPS Archive: Calhoun

Calhoun is the Naval Postgraduate School's public access digital repository for research materials and institutional publications created by the NPS community. Calhoun is named for Professor of Mathematics Guy K. Calhoun, NPS's first appointed -- and published -- scholarly author.

Dudley Knox Library / Naval Postgraduate School
411 Dyer Road / 1 University Circle
Monterey, California USA 93943

http://www.nps.edu/library

CONSTRUCTION OF A CARBON DIOXIDE TEA LASER

Douglas Harmon Barr

NAVAL POSTGRADUATE SCHOOL
Monterey, California

THESIS

CONSTRUCTION OF A CARBON DIOXIDE TEA LASER

by

Douglas Harmon Barr

Thesis Advisors: Fred R. Schwirzke and
Natale M. Ceglio

June 1972

Approved for public release; distribution unlimited

Construction of a Carbon Dioxide TEA Laser

by

Douglas Harmon Barr
Captain, United States Army
B.S., United States Military Academy, 1964

Submitted in partial fulfillment of the
requirements for the degree of

MASTER OF SCIENCE IN PHYSICS

from the

NAVAL POSTGRADUATE SCHOOL
June 1972

[illegible]

ABSTRACT

The recent development of CO_2 Transverse Excitation at Atmospheric Pressure (TEA) lasers has generated expanding interest and success due to their high pulsed power capabilities and simplicity of construction. We therefore decided to construct a CO_2 TEA laser because of the need for a high powered, pulsed, coherent radiation source with wave length near 10 microns to conduct absorption studies of laser-induced plasmas. It was decided that the constructed laser should have an output energy per pulse between 10 to 50 joules with a pulse time between 0.1 to 1.0 microseconds. This paper deals with the construction of that laser, and includes a discussion of the background and physics of operation of the CO_2 TEA laser.

TABLE OF CONTENTS

I. INTRODUCTION -- 4

II. CO_2 TEA LASER BACKGROUND --------------------------- 6

A. OLD METHOD OF OPERATION --------------------------- 6

B. TRANSVERSE EXCITATION METHOD ------------------- 8

III. PHYSICS OF THE CO_2 TEA LASER ---------------------- 13

A. VIBRATIONAL MODES ---------------------------------- 13

B. SELECTIVE EXCITATION PROCESS ------------------- 16

C. SELECTIVE DE-EXCITATION PROCESS --------------- 19

D. NON-RESONANT DE-EXCITATION ---------------------- 20

E. COMPETITION EFFECTS ------------------------------ 21

IV. CONSTRUCTION ------------------------------------- 25

A. MECHANICAL --------------------------------------- 25

B. ELECTRICAL -- 28

C. MIRRORS --- 32

V. CONCLUSIONS --------------------------------------- 37

A. RESULTS --- 37

B. EXPECTED RESULTS ---------------------------------- 37

C. POSSIBLE LASER TESTS ----------------------------- 39

FIGURES -- 41

BIBLIOGRAPHY -- 47

INITIAL DISTRIBUTION LIST --------------------------- 50

FORM DD 1473 -- 51

II. INTRODUCTION

Recently a need arose at the Naval Postgraduate School for a high powered, pulsed, coherent, radiation source with wavelength around 10 microns. Radiation at this wavelength can presumably heat plasmas to high temperatures effectively, and such a device was needed to do further absorption studies of laser radiation in a plasma. In view of the expanding interest and success being made in the development of TEA lasers at that time, and their apparent simplicity of construction, it was decided to construct a CO_2 TEA laser as a thesis project.

The term TEA Laser is an acronym for "Transverse Excitation at Atmospheric Pressure" Laser [20]. In general it implies that one is talking about gas lasers operating at or near atmospheric pressure with pumping electrodes situated transverse to the axis of the laser cavity, and that all these conditions are contrived in order to achieve high peak output power pulses. This type of laser has some marked advantages over solid-state type lasers which make it desirable for use at the school. CO_2 TEA laser efficiencies are typically higher, ranging from about 10 to 20 percent, compared to about 0.1 to 1.0 percent for most solid state types. As a result, higher output powers can be attained. Furthermore, the wavelength of operation is near 10.6 microns which is much longer than that for most solid state

lasers whose wavelength generally falls in the visible portion of the electromagnetic spectrum (e.g., for ruby lasers, $\lambda = 6943$ A°; for Nd, $\lambda = 1.06$ microns). The longer wavelength is more useful for heating and diagnostic studies of plasmas with densities in the range of 10^{15} to 10^{19} electrons per cubic centimeter. The plasma heating occurs by absorption of incident laser light, where the plasma absorption coefficient, K, at the frequency ν, is given by

$$K = \frac{1.17 \times 10^{-8}\, Z\, n_e^{2} \ln \Lambda}{3\nu^{2} (kT)^{3/2}} \qquad \frac{1}{\left[1 - (\nu_p^{2}/\nu^{2})\right]^{1/2}} \qquad (1)$$

where Z is the atomic number and $\ln \Lambda$ is the Coulomb logarithm [6]. Finally, this laser is less expensive to construct than a comparable solid state laser because the active medium consists of a gas rather than an expensive crystal with high optic qualities.

It was decided, therefore, that the laser should be a pulsed CO_2 TEA type emitting coherent, polarized radiation at 10.6 microns. The laser would be designed to achieve the following output characteristics:

OUTPUT ENERGY PER PULSE: 10-50 joules

PULSE TIME: 0.1 - 1.0 microseconds

PEAK OUTPUT POWER: at least 10 megawatts

MAXIMUM INPUT VOLTAGE: 60 kilovolts

DESIRED LASER EFFICIENCY: 5-10 percent

III. CO_2 TEA LASER BACKGROUND

A. OLD METHOD OF OPERATION

Until recently molecular gas lasers such as CO_2 had not been able to generate high peak powers because of their low density of active molecules compared to solid state materials. The old model for obtaining laser action consisted of placing the gas in a cylindrical or rectangular container inside of an optical cavity. Then the CO_2 molecules were excited to their upper vibrational levels by injecting energy through electrical discharge from electrodes located at each end of the container. For optimum continuous laser output, very low pressures (on the order of 1 torr) had to be maintained. In order to get reasonably high peak power pulses from this arrangement, Q-switching devices had to be employed. These devices were necessary for at least two reasons. First, the density of active molecules is about three orders of magnitude less than that for typical solid state lasers. Second, the photon energy per transition is from 10-20 times less due to the longer wavelengths involved. The coupling of these two factors means that at low pressures CO_2 cannot even approach the pulsed power capability of a comparable solid state laser.

In order to obtain high peak powers from CO_2 it becomes necessary to increase the gas molecule densities so that more laser transitions per unit time will be possible. This

means going to higher pressures and larger discharge volumes. High pressure operation, which will be defined as at or near atmospheric pressure, created additional problems however. As pressures rise larger voltages are needed to achieve breakdown. For example, at a pressure of one torr a CO_2 laser with an electrode gap of one meter would require a breakdown voltage on the order of 1.3 kilovolts; if that same laser were operated at atmospheric pressure, it would require a breakdown voltage on the order of 10^3 kilovolts, or one million volts. If these high voltages could be attained, the result would likely be an arc discharge resulting from high pressure ionization instabilities rather than the uniform volume discharge that is desired.

A uniform volume discharge is essential for high laser efficiency. The CO_2 molecules, which are evenly distributed throughout the cavity volume, are collisionally excited to their upper laser levels by inelastic collisions with electrons being accelerated from the cathode to the anode. Therefore, in order to get the maximum number of molecules excited it is necessary to achieve a uniform volume discharge of electrons in the laser cavity. Anything less than that produces inefficient collisional energy transfer and therefore reduced laser efficiency. Hence, the old model of a cylinder with electrodes at each end becomes impractical at high pressure because the voltages needed for discharge are too high, and any result would be an arc rather than a uniform volume discharge.

B. TRANSVERSE EXCITATION METHOD

To overcome the problems of high pressure operation the electrode geometry must be modified to achieve "transverse" rather than "longitudinal" excitation. Transverse excitation (TE) employs a short discharge length but a large area to achieve a large discharge volume. The method is better for several reasons. First, the high voltages needed to attain high pressure breakdown are applied over relatively short distances. This means low workable voltages can be used to obtain large discharge volumes at high pressures. For example, the electrode gap is expected to be from two to six centimeters. This gap will require a discharge voltage of from 20 to 60 kilovolts at atmospheric pressure, which is small compared to 10^3 kilovolts. Therefore, with a uniform discharge the result is greater laser energy produced by smaller voltages.

Another TE advantage leading to higher efficiency comes from the low discharge impedance inherent in a short electrode gap. Low impedance allows a very rapid injection of the excitation energy. (Injection times on the order of 10^{-6} to 10^{-7} seconds are expected.) The importance of rapid energy injection is due to the time scales for laser action. To achieve high laser efficiency the excitation pulse width must be small compared to the collisional lifetime of CO_2 in its upper laser level. This is so that each molecule will spend most of its time in the upper state maintaining the population inversion until conditions are favorable for

rapid depopulation. The molecule must spend minimal time in the lower levels and in the process of being excited to the upper level. Since the CO_2 upper level collisional lifetime at one atmosphere is near 10^{-5} seconds, the transverse excitation time is significantly less. Therefore, transverse excitation is well suited for rapid energy injection which enhances laser efficiency.

The rapid discharge nature also eliminates the need for Q-switching devices to achieve giant power pulses. Natural giant pulses automatically occur from rapid energy injection by means of a phenomenon called "gain switching." To realize how gain switching occurs, consider the sequence of diagrams illustrated in figure 1. Graphs (a) and (b) depict the input voltage and current pulses formed as a high voltage capacitor bank is suddenly discharged across a low impedance transverse excitation electrode gap. The voltage and current pulses are similar in form, and both are less than a microsecond wide. The current pulse lags the voltage by a small but finite breakdown time (due to the time it takes for electrons to form) in the gap. The gain (c) builds up during the excitation pulse and reaches its maximum near the end of it. The gain has reached its maximum in a time less than the mean lifetime of the molecules existing in their excited state ($\tau_{coll} \approx 10^{-5}$ sec). This means nearly all available molecules have been kicked up to their upper level before many have had a chance to depopulate. This situation produces a nearly ideal population inversion. A

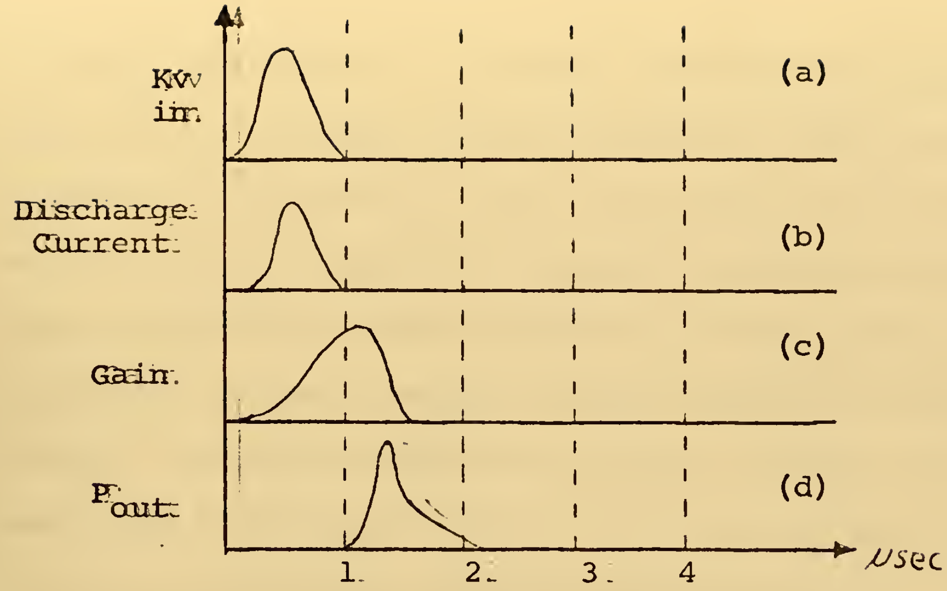

Figure 1.

giant laser pulse will follow as all the excited molecules rapidly cascade downward to their lower level, emitting intense laser radiation over a short time. Previously, Q-switching devices had to be employed to attain high power pulses (increased by a factor of roughly 10^3). With TE methods, however, these giant power pulses become an automatic result by means of the gain switching phenomenon.

A final big advantage of transverse excitation is that it facilitates the use of double-discharge preionization techniques to attain uniform volume discharges. With all the advantages mentioned, transverse excitation will not yield the uniform volume discharge needed for high efficiency. Therefore some means must be used to spread the discharge uniformly. Preionization by double discharge utilizes a series of insulated "trigger" electrodes, in close proximity to the cathode, whose potential is essentially that of the anode. When a high voltage pulse is applied to the anode,

it first initiates a low energy cathode-to-trigger discharge sufficient to create a uniform sheet of electrons around the cathode. Subsequently, when the voltage pulse reaches higher values, the main cathode to anode discharge takes place. The preionization effect spreads uniformly this ensuing discharge so that a uniform volume discharge results. The trigger electrodes apparently do not increase the total number of discharge electrons, but serve rather effectively to spread them into a uniform volume discharge. This technique minimizes the effects of electrode irregularities along with the tendency to generate concentrated arcing. With proper application of these preionization techniques, laser efficiencies can be enhanced from around 3 percent to the 10-20 percent range.

In summary, the output of the CO_2 laser is immensely increased by operating at high pressure (atmospheric) with transverse excitation methods. Such operation, referred to as "Transverse Excitation at Atmospheric Pressure," or the TEA mode, has the aforementioned advantages:

1. Greater molecule density and therefore greater available energy density.

2. Greater active volume due to large electrode surface areas.

3. Relatively low working voltages required to generate large fields due to short discharge gap.

4. Higher laser efficiencies due to:

    a. Rapid energy injection

b. Pre-ionization techniques

5. Giant pulses without Q-switching due to gain switching.

III. PHYSICS OF THE CO_2 TEA LASER

A. VIBRATIONAL MODES

In order to understand the physics of CO_2 laser action, one must look first at the CO_2 molecule itself (Figure 2). The CO_2 molecule is a linear, symmetric, triatomic molecule with three degrees of vibrational freedom. Associated with these degrees of freedom are three separate vibrational modes. In the first mode, called the "symmetric stretch," the two oxygen atoms vibrate along the internuclear axis in a symmetric fashion (MODE 1). For future reference this mode will be designated as $(\nu_1, 0, 0)$. In the second vibrational mode, or "bending mode," designated $(0, \nu_2, 0)$, the two oxygen atoms oscillate perpendicular to the internuclear axis as shown (MODE 2). In the final mode or "asymmetric stretch," designated $(0, 0, \nu_3)$, all three atoms oscillate in an asymmetric fashion along the internuclear axis (MODE 3) [16]. To a first approximation, these three modes can be considered as independent of each other. Therefore, the total vibrational state of the CO_2 molecule at any time is essentially a linear combination of the three modes, since it can vibrate in all three modes at once. The total state is described by the three vibrational quantum numbers (v_1, v_2, v_3), and the vibrational mechanical energy is given by the harmonic oscillator energy equation. This could be written as:

$$E_{\text{vib total}} = \sum_{n=1}^{3} E_{\text{vib}_n} = (v_1+\tfrac{1}{2})hfo_1 + (v_2+\tfrac{1}{2})hfo_2 + (v_3+\tfrac{1}{2})hfo_3 \qquad (2)$$

where fo_n is the natural frequency of oscillation in the n^{th} mode.

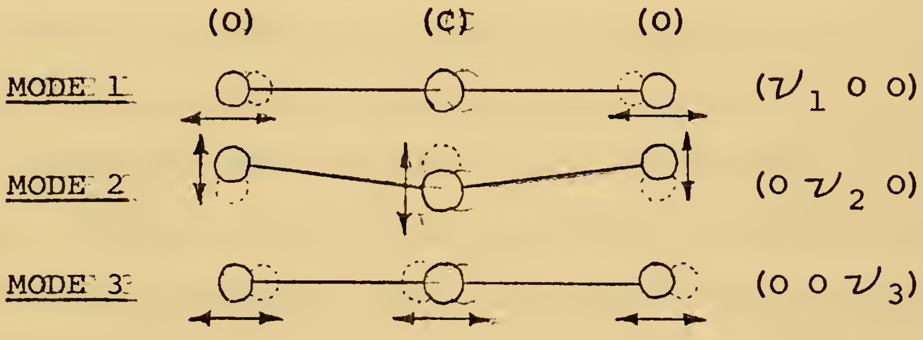

Figure 2.

The energy level diagram for the low lying vibrational states of CO_2 is shown in figure 3. Rotational levels for each vibrational state are not shown in order to keep the diagram simple. By nature, vibrational levels are nearly evenly spaced. Each mode forms an almost equally spaced ladder of energy levels. The energy spacing between the ν_1 levels is approximately 0.17 electron volts; between the ν_2 levels it is approximately 0.08 electron volts, and for the ν_3 levels the energy gap corresponds to about 0.29 electron volts. (Rotational levels are much more closely and unevenly spaced with energy gaps of 0.001 electron volts and less.)

The CO_2 (001) level is the desirable upper laser level. The (100) and (020) levels form the lower laser levels.

The excitation process involves electron-molecule inelastic collisions that excite the CO_2 molecule ultimately to the (001) level. From here the molecule undergoes the (001)-(100) downward transition, emitting infrared radiation near 10.6 microns. The other possible transition from (001) to (020) emits radiation near 9.6 microns, but due to a larger emission probability, the (001)-(100) transitions at 10.6 microns are about ten times stronger than those at 9.6 microns. Therefore, only the 10.6 micron transition will be considered. After the laser transition at 10.6 microns, the CO_2 molecule then undergoes radiative and collision-induced transitions to the (010) level, and then to ground level. At this point it is available for excitation again to the upper level.

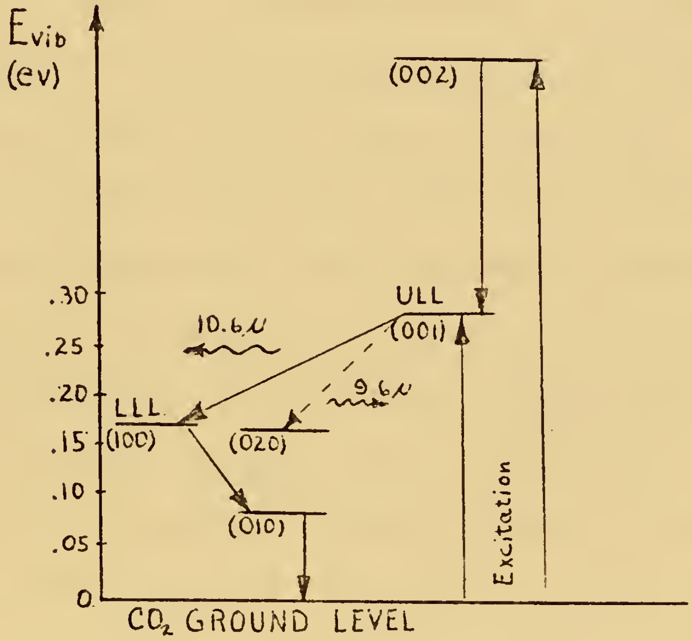

Figure 3.

The quantum efficiency is defined as the laser photon energy divided by the upper-laser-level excitation energy.

For CO_2, it is nearly 41 percent. This figure is very high compared to most solid state and atomic gas lasers whose quantum efficiencies normally fall in the range of 1 to 10 percent. This high quantum efficiency makes it possible to attain high laser efficiencies provided that the input energy is efficiently transferred to the desired upper level rather than distributed to extraneous levels. Such a process of "selective excitation" is possible in the CO_2 laser. It is this selective excitation coupled with the high quantum efficiency that enables one to attain laser efficiencies as high as 10 to 20 percent.

B. SELECTIVE EXCITATION PROCESS

Selective excitation is a collision-dominated process. In the CO_2 TEA laser, energy injection is by means of an electric discharge that creates a (uniform) flux of electrons whose average energy is near one electron volt. A large number of inelastic collisions take place between the accelerated electrons and the existing CO_2 molecules, causing the molecules to be excited to various vibrational levels. At one electron volt, the electrons preferentially excite CO_2 to the $(0\ 0\ \nu_3)$ levels, i.e., to the nearly equally spaced levels of the mode 3 energy ladder. Selective excitation becomes possible because the $(0\ 0\ \nu_3)$ levels are almost equally spaced. Collisions between $CO_2(00\nu_3)$ molecules with those at ground level result in an efficient transfer of vibrational energy from excited molecules to

unexcited molecules, i.e.,

$$CO_2(00\nu_3) + CO_2(000) \longrightarrow CO_2(00\nu_3-1) + CO_2(001) \qquad (3)$$

Similar processes follow that bring the $(00\nu_3)$ molecules down the ladder to the (001) level while simultaneously kicking ground state molecules into the (001) level by collisional transfer of energy. This mechanism is resonant in the sense that there is an efficient redistribution of the excited molecule energy to the (001) level with very little loss of the total internal energy of the system. The efficiency of redistributing the $CO_2(00\nu_3)$ molecule energy into the upper laser level is high. This fact implies that the excitation mechanism is considerably effective.

Nevertheless, electron impact excitation in pure CO_2 gas cannot by itself attain the needed selective excitation for high efficiencies; normally there are a good number of molecules excited to upper levels other than in the $(00\nu_3)$ mode. These molecules produce wasted energy that reduces laser efficiency. Another form of selective excitation is needed to complement the process previously mentioned. This is done by adding nitrogen gas to the carbon dioxide. The usefulness of N_2 can be seen from its energy level diagram for the low lying vibrational levels of its electronic ground state (Figure 4). Since N_2 is a diatomic molecule, it has only one degree of vibrational freedom (along the internuclear axis). Therefore, only one quantum number (v)

is needed to describe completely the vibrational state of the molecule. It turns out that the energy levels of N_2 coincide almost exactly with those of the $(00\nu_3)$ mode of CO_2. Therefore efficient collisional energy transfer is possible. As with CO_2, the N_2 molecules become collisionally excited to their upper vibrational levels by electron impact.

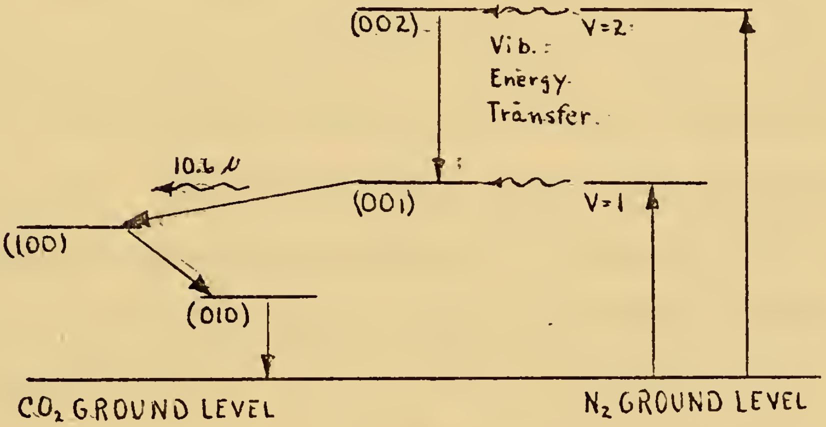

Figure 4.

Since the excitation energy of $N_2(v=1)$ nearly equals that of $CO_2(001)$, an efficient transfer of vibrational energy to CO_2 is possible as follows:

$$N_2(v=1) + CO_2(000) \rightarrow N_2(v=0) + CO_2(001) \tag{4}$$

In a more general sense, the reaction would be of the form:

$$N_2(v=v') + CO_2(000) \rightarrow N_2(v=v'-1) + CO_2(001). \tag{5}$$

This quantum transfer of energy can be recycled again and again so that all N_2 vibrational levels contribute to the redistribution of vibrational energy. Because of the resonant nature of the process, the selective excitation of CO_2 to the (001) level becomes even more dominant.

A further resonant mechanism exists because of the close coincidence of N_2 and $CO_2(00\nu_3)$ energy levels. In collisions involving $N_2(v=v'')$ and $CO_2(000)$, efficient vibrational energy transfer can take place in the following fashion:

$$N_2(v=v'') + CO_2(000) \rightarrow N_2(v=0) + CO_2(00\nu_3=v'). \qquad (6)$$

Once this total energy exchange takes place the excited CO_2 molecules can then redistribute their energy to the (001) level by the resonant process previously described in Equation (3). The final result of all three selective excitation modes is an efficient redistribution of the total molecule vibrational energy into the desired upper laser level (001).

C. SELECTIVE DE-EXCITATION PROCESS

Once the CO_2 molecule is selectively excited to the (001) level, it can emit a laser photon at 10.6 microns as it de-excites to the (100) level. From this point it must return (rapidly) to ground state before it can be used again for producing a laser photon. The molecules at the (100) level are de-excited essentially by collisions with other molecules. Here again the possibility of resonant vibrational energy transfer plays an important role that allows a "selective de-excitation" process to occur. From the CO_2 energy level diagram one can see that the lower laser level (100) has nearly twice the energy required to excite CO_2 to the (010) level. Therefore, if a CO_2 (100) molecule collides

with a $CO_2(000)$ molecule, the vibrational energy can be efficiently redistributed between the two by exciting both to the (010) level, i.e.:

$$CO_2(100) + CO_2(000) \longrightarrow 2\,CO_2(010) \qquad (7)$$

Here again a resonant-like process exists in the sense that there is an efficient transfer of vibrational energy by collisions so that most CO_2 molecules tend to redistribute to the (010) level.

D. NONRESONANT DE-EXCITATION

The de-excitation process is not complete, however, until the CO_2 molecule ends up in its ground state. The de-excitation of CO_2 from (010) to (000) is also dominated by collisions, but now they are "nonresonant" ones because the energy of $CO_2(010)$ is converted to kinetic energy of the background molecules, or heat energy of the container walls. Because of the nonresonant nature of this phase, the transfer of $CO_2(010)$ to ground level can be slow and cause a bottleneck in the overall laser cycle. The result may be reduced efficiency and less energy out. To avoid this bottleneck one must somehow increase the non-resonant collision rate. This rate depends on the nature of the background particles. CO_2 molecules, for example, have about 100 de-exciting collisions per torr per second, while helium atoms have on the order of 4000 collisions per torr per second [17]. Therefore, one can reduce the bottleneck and increase laser efficiency by adding a gas like helium to the CO_2 mixture.

In summary, by adding N_2 and H_e gas, the CO_2 laser efficiency can be increased by means of two effects:

(1) An increased selective excitation rate of CO_2 to the (001) level resulting from increased N_2 - CO_2 collision rates.

(2) An increased (nonresonant) de-excitation rate of CO_2(010) to ground state resulting from increased H_e - CO_2 collision rates.

Typical CO_2 : N_2 : H_e mixture ratios run in the vicinity of 1 : 1 : 12 (flowing) and have produced laser efficiencies up to 20 percent.

E. COMPETITION EFFECTS

To this point, no mention has been made of the various rotational levels that produce the many possible P and R branch transitions. One might think that the energy output would occur at many frequencies corresponding to these discrete P and R branch transitions. It turns out that this is not the case. In spite of the fact that the (001) - (100) vibrational transition contains many possible P and R branch transitions, the output can be essentially monochromatic at 10.5915 microns. This specific wavelength corresponds to a single P branch transition, namely P(20). The unique nature of the output radiation can be explained in terms of "competition effects" between the various P and R branch transitions.

During laser action, the CO_2 molecules are essentially at room temperature and have a mean kinetic energy of about

.025 electron volts. Since energy spacings between vibrational levels are in the range of 0.1 to 1.0 electron volts, while rotational energy spacings are no larger than 0.001 electron volts, it is generally true that $\Delta E_{vib} \gg K.E._{molecule} \gg \Delta E_{Rot}$. As a result the CO_2 molecule can jump around easily from one rotational level to the next; it does so at a high frequency, called the thermalization rate. The rotational thermalization rate at room temperature is approximately 10^7 hops per second. Since the time between hops is roughly 10^{-7} seconds, these levels rapidly become thermalized in a Boltzmann distribution among the various rotational levels of a given vibrational level. On the other hand the vibrational thermalization rate is relatively small at 10^3 hops per second. This rate is associated with a mean vibrational lifetime of 10^{-3} seconds, which is very long in terms of the scale on which laser events take place. Laser action takes place in 10^{-6} seconds or less. Therefore, the molecules will remain in their selectively excited vibrational level (001) but will become thermalized in their rotational levels about some peak level (Figure 5). This peak level is the J = 19 rotational level

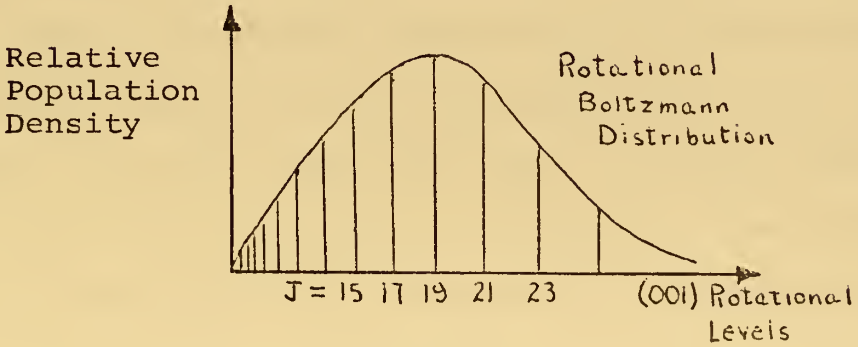

Figure 5.

of the (001) vibrational level. The dominant transition occurs between (001) J = 19 and (100) J = 20 and is labeled the P(20) transition (Figure 6).

Because the rotational levels become rapidly thermalized into a Boltzmann distribution, any change in the population density of one level changes the population density of all other levels in a fashion that will tend to maintain the original Boltzmann distribution. The transition with the highest gain, P(20), will begin oscillating first. When this occurs the rate at which molecules are drained from the J = 19 level increases due to the resulting stimulated emissions on the P(20) transition. The requirement to maintain the Boltzmann distribution, however, will cause a transfer of molecules from other rotational levels to the J = 19. Therefore, the population density of all other rotational levels decreases even through laser oscillation on P(20) drains molecules from the J = 19 level. A strong competition among possible laser transitions can exist from this situation, and usually one P branch transition dominates. In this case the dominant transition is P(20) at 10.5915 microns.

As a matter of interest, oscillation in less dominant P and R branch transitions can be produced if there exists enough gain for that transition, and if stronger transitions are prevented from oscillating. This can be done by means of a wave length selecting mechanism such as a grating or prism. Because of the strong competition effects, one can

obtain roughly the same amount of output power on any selected transition using wave length selecting methods.

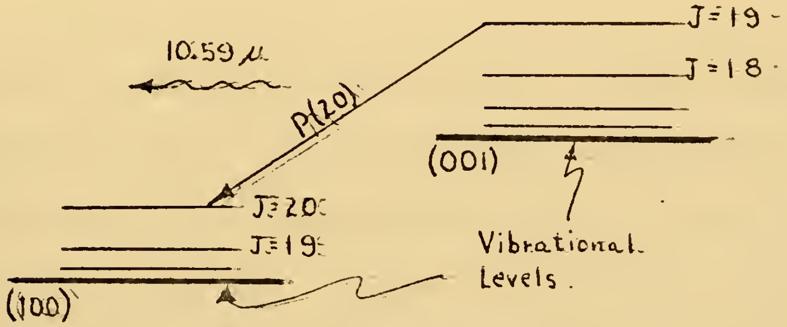

Figure 6.1.

IV. CONSTRUCTION

A. MECHANICAL

The overall laser system consists of a rectangular container filled with a mixture of carbon dioxide, nitrogen, and helium gases, and with large area electrodes located transverse to the longitudinal axis of the container for electrical pumping. Brewster windows are at each end, and outside of these are end mirrors that form the optical resonator. The laser electrodes are connected to a 60 kilovolt Marx Bank impulse generator which supplies the input energy.

The laser box (Figure 9) is 40 inches long, 12 inches wide, 6 inches high, and was made of 1 inch thick acrylic lucite walls and a 1 inch thick aluminum bottom plate. The walls were fastened by 1½ inch screws, and so no attempt was made to make the chamber vacuum tight. Rectangular laser portals (5 x 1-3/4 inch) were cut at each end, and lucite sidewalls were attached to form Brewster window mounts at the Brewster angle of 56° 19' with respect to the end wall (Figure 12). The Brewster windows consist of 2 polished NaCl crystals (5½ x 5½ x 3/8 inch) attached to the Brewster window mounts with silicon glue. The box itself rests on an optical bench 160 centimeters in length which is securely attached to a rigid table.

Inside the laser box is located the electrode assembly (Figure 10), consisting of an anode, a cathode, and trigger

electrodes. The anode consists of a ¼ inch copper plate 38 inches long and 5 inches wide. The corners were rounded and all edges were smoothed to minimize arcing effects. It was braced by two 37 inch lengths of 1 inch thick lucite. The lucite braces run nearly the length of the laser and were fastened securely to the top of the laser box. Four sections of threaded copper rods (1 inch O.D., 3-3/8 inch length) were used for electrical input to the anode. These sections were soldered to the top side of the anode; they also function as bolts through the top of the box to secure the anode to it. The combination of bolts and lucite braces insured that the anode was rigidly fixed to the top of the box and accurately aligned.

The cathode consists of a copper plate that is 1½ inches thick, 36 inches long, 4 inches wide, and contains 115 triangular ridges and grooves running transverse to the length, across the 4 inch width (Figure 11). The grooves were cut 3/8 inch into the plate and are separated by 5/16 inch. The apex of each ridge forms a 45^{o} angle; all corners were rounded to minimize arcing effects. The cathode structure was bolted to the 1 inch thick aluminum base plate which is 48 inches long and 12 inches wide. The base plate was, in turn, secured to the optical bench so that the bench would be at ground potential along with the cathode and base plate. The cathode was secured to the base plate by six threaded copper rods (1 inch O.D.) soldered to the bottom of the cathode. These rods are 2½ inches long and serve both

as bolts to the aluminum base plate and as the electrical feed connectors between the cathode and ground potential for the impulse generator.

The trigger electrodes consist of 115 pyrex capillary tubes (7/32 inch O.D., 7 inch length), each containing a 9 inch nichrome trigger wire (.01 inch O.D.) within. The wires were sealed in the glass at the far end, and had two 90 degree bends at the exposed end to facilitate connection to an electrical terminal located near the wall of the laser box (Figure 10). Each capillary tube with trigger wire was set in one of the 115 cathode grooves and spot glued in place so that each wire rested at nearly the same level as the top edge of the copper ridge. The nichrome wires were soldered to a copper terminal (½ x ¼ x 36 inches) running the length of the cathode at a distance of 2¼ inches from its nearest edge. The copper terminal was connected to the anode through a capacitor.

The electrode assembly was constructed so that the gap between anode and cathode could be varied from a minimum of 2 centimeters to any maximum value desired. The trigger electrodes remain fixed, however. Increasing the electrode gap consists of removing the lucite box and attached anode from the aluminum base plate, and placing a lucite gasket of the desired thickness on the base plate. The laser box and anode are then remounted to the base plate and gasket at a new height dictated by the thickness of the lucite gasket. It is anticipated that electrode gaps between 2 and 6 centimeters will be used.

The carbon dioxide, nitrogen, and helium will come pre-mixed in a single supply tank. The mixture ratio will be 15:10:75 initially. This pre-mixed method is merely an expedient, however, to obtain successful laser action as early as possible. Once this is achieved, the gas hookups will be modified to accommodate separate tanks of each type of gas. Then gas mixture ratios and flow rates can be varied to test the laser action as a function of these parameters. Also new gases can be introduced in combination with carbon dioxide to test their effects on laser action. These procedures will call for some additional valves and gas flow meters to regulate the mixture ratios. Also a gas mixing tank will be used prior to introducing the gases into the laser cavity. Additional gas inlet and outlet holes will have to be made in the laser box to attain a desirable flow pattern transverse to the laser axis and the discharge path.

B. ELECTRICAL

The input energy will be by an electrical discharge across the electrodes, produced by a high voltage short duration pulse. The discharge voltage required to attain the desired breakdown at atmospheric pressure will be between roughly 20 and 60 kilovolts for electrode spacings of 2 to 6 centimeters, respectively. The input pulse duration will be on the order of a microsecond. A three stage marx bank impulse generator fed by a 20 kilovolt, 15 milliamp DC power supply will constitute the electrical power source (Figure 13).

A marx type generator is an excellent method of attaining the high voltage, short pulsed energy injection required to operate a double-discharge TEA laser. A simple schematic for a marx generator is shown in Figure 7. The marx system achieves impulse voltage multiplication by charging capacitor stages in parallel and discharging them in series. The capacitor stages are connected in series by switching spark gaps. One of the switches is in the form of a triggering spark gap with external ignition means. If C_N is the required capacitance of the total network storage capacitor when discharged, then each capacitor discharged in series (C) must have a value nC_N, where n is the number of stages. In Figure 7, n=3 and so each of the 3 capacitors must have a value of $C=3C_N$. The isolating elements (R) prevent the capacitors from being short circuited through the gaps during the pulse, and so they must have a sufficient value to do so.

The main advantage of the marx system is that voltage multiplication is achieved. The marx circuit gives higher output voltage than a comparable parallel bank arrangement with the same stored energy by rearranging the bank into n equivalent circuits. Ideally, the voltage out will be nV_{in}, giving an n-fold voltage multiplication. In practice, however, it is expected that roughly 10 percent of the voltage will be lost due to currents flowing through the isolating elements. Because of the voltage multiplication the direct current source required is relatively small, and also less insulation is required in the circuit compared to the

equivalent LCR circuit. A further advantage is that it eliminates the need for a transformer, which makes it good for experimental purposes. The main disadvantage is that it requires larger individual capacitors since each must have a value $C = nC_N$ where C_N is the desired capacitance of the network storage bank under discharge.

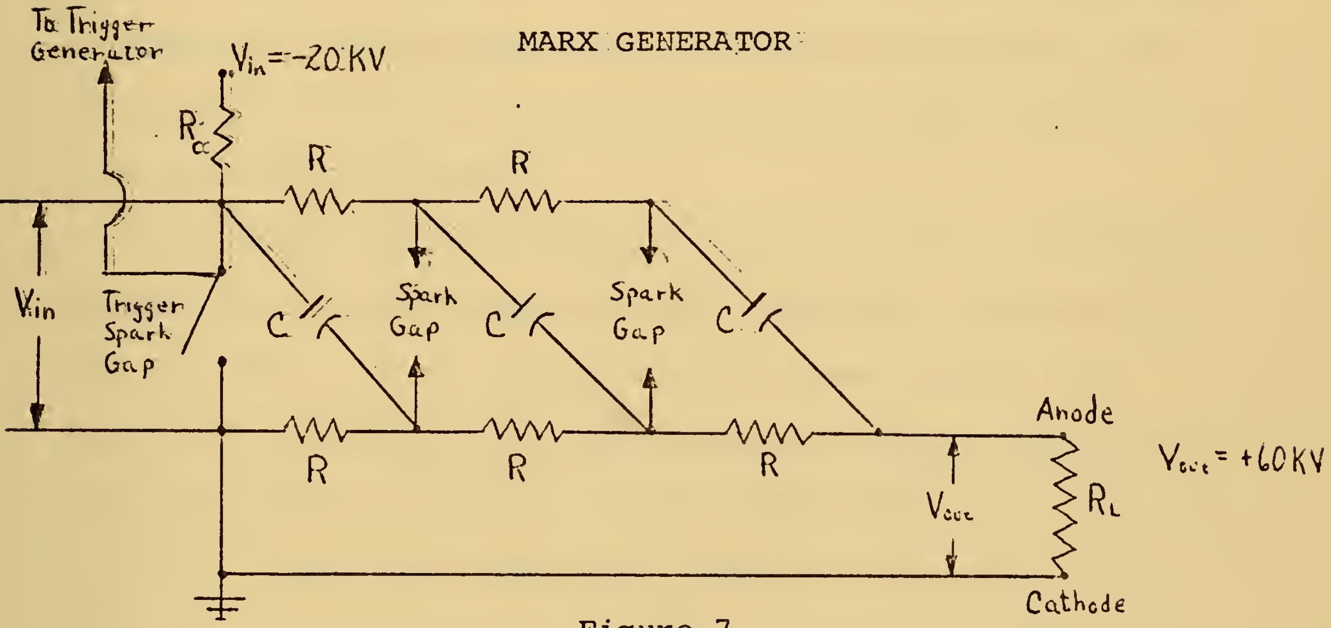
MARX GENERATOR

Figure 7.

The particular marx generator used (Tachisto, Inc., Model MC-3, No. 14) is a three stage device designed for a maximum charging voltage of 20 kilovolts and a maximum output voltage of 60 kilovolts. A safe pulse rate is 5 pulses per second, although pulse rates up to 12 pulses per second can be tolerated for short periods of time. The capacitance per stage is 0.5 microfarads (with a possibility of going to 0.75 microfarads per stage) producing an overall network capacitance of $C_N = 0.167$ microfarads during discharge. The isolating elements are 333 ohm resistors.

A charging impedance (R_c) must be placed in series with the 20 kilovolt DC charging line to limit the current drawn from this power supply. A power resistor is the simplest such charging element, provided it is satisfactory from the standpoint of power dissipation, current and voltage rating of the power supply, and desired repetition rate. The main disadvantage of such resistive charging is that the maximum efficiency is 50 percent. Resistive charging should prove satisfactory at least initially, however, since low repetition rates will be used.

The choice of the charging resistance value is determined by two conflicting factors, pulse repetition rate and maximum allowable current drain from the power supply. As previously mentioned, the capacitors are charged in parallel and discharged in series, and the capacitance per stage must be nC_N. Therefore, during the parallel charging, a unit with n stages represents an equivalent capacitance to the power supply of $C_{eq} = n(nC_N) = n^2C_N$, and the time constant for charging through a resistor R_c is $\tau = R_c C_{eq}$. It is desirable to have an interpulse period of at least 3τ so that the capacitors can become charged to 95 percent of V_{in}. Therefore for f pulses per second, the repetition rate criterion is that

$$R_c \leq \left[3fC_{eq}\right]^{-1} \qquad (8)$$

At the moment after firing, the marx generator looks like a short circuit to the power supply, so that the instantaneous current drawn will be

$$i = V_{in}/R_c \quad (9)$$

If this current is limited to the value i_{max} by the power supply, then the maximum allowable current criterion is that $i \leqslant i_{max}$ which places a lower limit on R_c such that

$$R_c \geq V_{in}/i_{max} \quad (10)$$

Actually this limit can be exceeded somewhat due to the power supply output capacitance, charging lead inductance, and the non-zero response time of system circuit breakers.

Assuming that both equations (8) and (10) hold, the necessary power supply current for the desired repetition rate f is

$$i_{max} = 3V_{in} C_{eq} f \quad (11)$$

For the 15 milliamp, 20 kilovolt power supply on hand and the 1.5 microfarad charging capacitance, the repetition rate should be no greater than one pulse per six seconds. To increase to 10 pulses per second will require increasing the charging current by a factor of 60.

C. MIRRORS

The optical resonator consists of two mirrors, one placed at each end of the laser box outside each Brewster window. The back-end mirror must be totally reflecting while the front-end or output mirror must be partially transmitting to let a certain fraction of the laser energy out. Past CO_2 TEA laser studies indicated that effective laser action could be realized by using output mirrors with a transmission coefficient in the range of .15 to .20.

There are two possible methods for achieving output coupling of energy with partial transmitting output mirrors. The first is to use a solid-back mirror whose transmission coefficient is sufficient to achieve optimum output without unduly damping laser oscillation in the cavity. This method was ruled out initially due to the high cost of such mirrors. The second method uses small holes placed in a totally reflecting mirror to achieve output coupling. This approach was chosen initially because it is less expensive and can be equally effective provided the gain is high and the hole size is small compared to the mode spot size. For example, if a particular mode has one of its maxima fall on a mirror hole, that mode will suffer increased loss; if hole size $\geq 0.2 \times$ spot size, losses due to the hole will probably be sufficient to produce a round trip gain for that mode less than one [15]. In this case the mode will no longer oscillate. Therefore, the hole size as well as hole pattern becomes an important consideration when employing this type of output coupling.

The mirror design was based on the requirement for a stable resonator to keep the energy loss per round trip small. Also a system insensitive to misalignment was desired to minimize losses from slight errors in mirror alignment. The stability criterion is that:

$$0 \leq g_1 g_2 \leq 1 \quad \text{(stable resonators)}$$

where $g \equiv 1 - L/R$, L is the resonator length and R is the mirror radius of curvature. This criterion can be

represented by the stability diagram (Figure 8), where any optical resonator can be depicted by a point in the g_1g_2 plane. Only those points falling in the shaded portion of the diagram correspond to stable resonators. Points lying outside the shaded portion correspond to unstable resonators. Hence, the first requirement for a stable resonator is met for any value $0 \leq g_1g_2 \leq 1$. Furthermore the line defined by $g_1 = g_2$ represents the least loss line, or the locus of points least sensitive to horizontal and angular misalignment; diffraction losses increase with departure from this line [10]. Therefore losses from misalignment should be minimized for points along the $g_1 = g_2$ line in the broadest shaded portion (designated by asterisks). These points, corresponding to $g = \pm 0.5$, appear to determine the best conditions for maximum stability and minimum loss [24]. For these values the radii of curvature turn out to be $R_1=R_2=2L$, or $R_1=R_2=\frac{2}{3}L$.

From this analysis it was decided to use symmetric, gold coated mirrors initially, whose radii of curvature are $R_1=R_2=\frac{2}{3}L = 1$ meter. Output coupling would be achieved by a series of evenly spaced holes with diameters of 0.334 millimeters. Additional mirrors with varying hole patterns and diameters would be tested later to determine their effects on laser output.

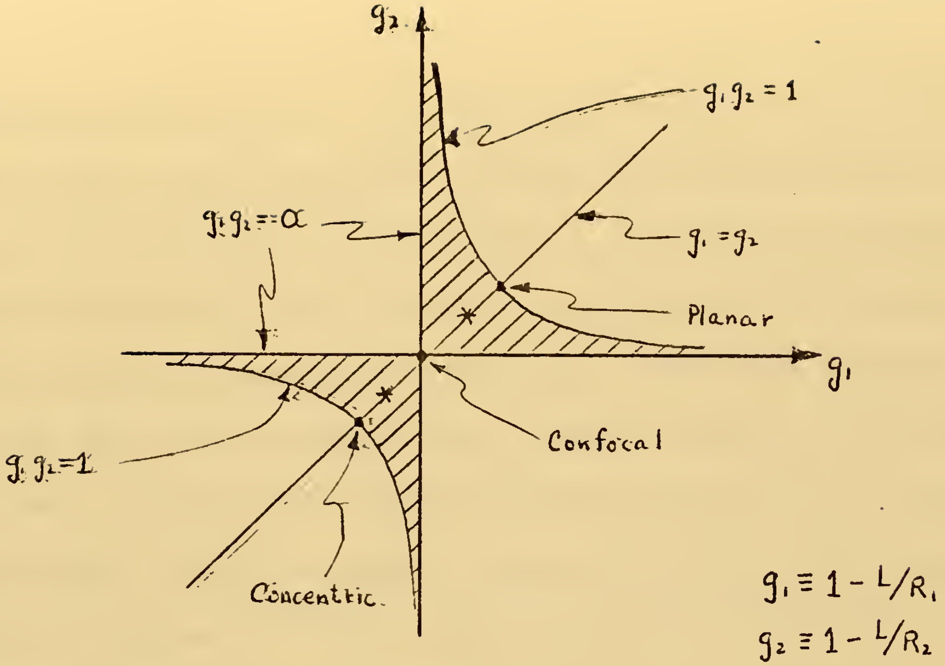

Figure 8.

Figure 14 depicts one such mirror configuration consisting of 287 holes (D=0.334mm) symmetrically placed about the horizontal and vertical axes of a polished, gold-coated aluminum plate five inches square with a radius of curvature of one meter. The spacing between holes is 0.10 inch. The hole size was derived from the general principles to optimize output coupling. They indicate that any mode having one of its maximum fall on a hole position will experience increased loss due to that hole; if the loss is sufficiently large for the total round trip gain of that mode to become less than one, the mode will no longer oscillate [18], [19]. Although the mode pattern inside the laser cavity will likely consist of a multitude of different modes combined, if one considers a single gaussian mode for the cavity and uses as a guide that the hole area must be less than 0.2 times the gaussian spot area, one can arrive at an approximate upper limit to

the tolerable hole size. The gaussian hole size can be calculated for this symmetrical resonator and turns out to be about 4.6 millimeters in diameter. Therefore an approximate upper limit for hole size for a single gaussian mode would be 2.05 millimeters in diameter. One might expect, then, that any hole diameter less than or equal to one millimeter surely would not degrade the gain unduly for a single gaussian mode. It is expected, therefore, that the mirror depicted in Figure 14, with hole diameter of 0.334 mm, will provide adequate output coupling of the laser energy.

VI. CONCLUSIONS

A. RESULTS

No results have been obtained yet because the laser is still in the construction phase.

B. EXPECTED RESULTS

1. Laser efficiency is expected to be at least 5 percent initially, and may very well approach 10 to 15 percent as tests continue and design problems are eliminated.

2. Energy per pulse out is expected to be near 10 joules initially. This figure is based on an energy input of between 200 and 300 joules per pulse, and an efficiency of 5 percent. The maximum possible energy input with the present power supply ($C_{eq} = 0.167$ f, $V_{gap} = 60$ KVolts) is 300 joules, neglecting losses, and so 200 joules may be a more accurate working figure. It is possible the output energy could be as high as 50 joules with the present power supply if laser efficiency is higher than 5 percent. For later experiments, the discharge capacitance may be increased to attain even higher output energy.

3. The energy pulse is expected to have a duration of between 0.1 and 1.0 microseconds. Therefore the peak power per pulse is expected to be between 10 to 100 megawatts.

4. The pulse repetition rate initially will be no greater than one pulse per 6 seconds. This requirement is

due mainly to the magnitude of the charging resistance (R_C = 1 megaohm) between the 20 kilovolt power supply and the marx generator. The charging time constant is 1.5 seconds, and so it will take roughly 6 seconds to achieve a full charge on the discharge capacitor bank.

5. Gain studies will be performed to determine the gain along the laser cavity length. It is expected that gain will be in the neighborhood of 3 percent per centimeter once efficient laser operation is established [7].

6. Time response studies of discharge voltage, current, and energy out will be made.

Measurement of the output power will be by means of a germanium photon drag detector, Model 7411, serial number 118 manufactured by Rofin Ltd., of England.

This device is designed for use with high power pulsed outputs obtained from Q-switched or TEA CO_2 lasers at 10.6 microns. It has a response time of less than one nanosecond from 10 percent to 90 percent of peak, and a responsivity of 0.18 ± .01 millivolts per kilowatt. The detector area is 4 square millimeters, and it can withstand pulsed powers up to 10 megawatts per square centimeter. The unit operates at room temperature and without amplifier.

The photon drag principle is based on the transfer of momentum from incident photons to free electrons and holes in a doped germanium rod. As incident radiation enters and passes through the doped crystal, the photons transfer their momentum to free carriers in the germanium conduction band.

The carriers with transferred momentum are then driven down the rod. The free carrier displacement creates a temporary induced electric field proportional to the intensity of the incident radiation. This field produces a voltage gradient which can be amplified or fed directly to an oscilloscope for measurement. The governing expression for the open circuit voltage induced by this process (V) in a photon drag detector is

$$V = -\frac{W(\rho\mu)(1-R)}{Ac} \qquad (12)$$

where W is the incident radiation intensity in watts, ρ is the resistivity of the sample, μ is the mobility of the carriers, A is the detector area, R is the sample reflection coefficient, and c is the speed of light [11]. This expression is valid only for a heavily doped semiconductor such as germanium. It is not valid for near-intrinsic materials, or when absorption by other than free carriers, such as phonons, is significant. By applying this relation to voltages obtained by photon drag measurements, one can determine the incident radiation intensity in watts.

C. POSSIBLE LASER TESTS

Tests will be made to determine the results listed in part B above. Further tests may possibly be made later to determine how these results vary as the following parameters are changed:

1. Electrodes:

   a. Vary the material.

   b. Change the geometry and double-discharge technique.

   c. Vary the electrode gap.

   d. Try coating the cathode surface to change the electron work functions.

2. Energy Input:

   Vary the input energy by means of changing the electrode gap and capacitor bank size.

3. Mirror Configuration:

   a. Vary the output coupling by changing the number, pattern, and size of mirror holes.

   b. Vary the surface coating material.

   c. Vary the mirror radii of curvature.

4. Gas Mixture:

   a. Vary the gas mixture ratios.

   b. Introduce new gas combinations.

5. External Ionization Source:

   a. Induce preionization by a radioactive source.

   b. Induce preionization by electron beam.

6. Scaling:

   Increase the laser to larger dimensions. It appears that CO_2 TEA Lasers can be scaled up to larger dimensions without appreciable loss of performance per unit volume.

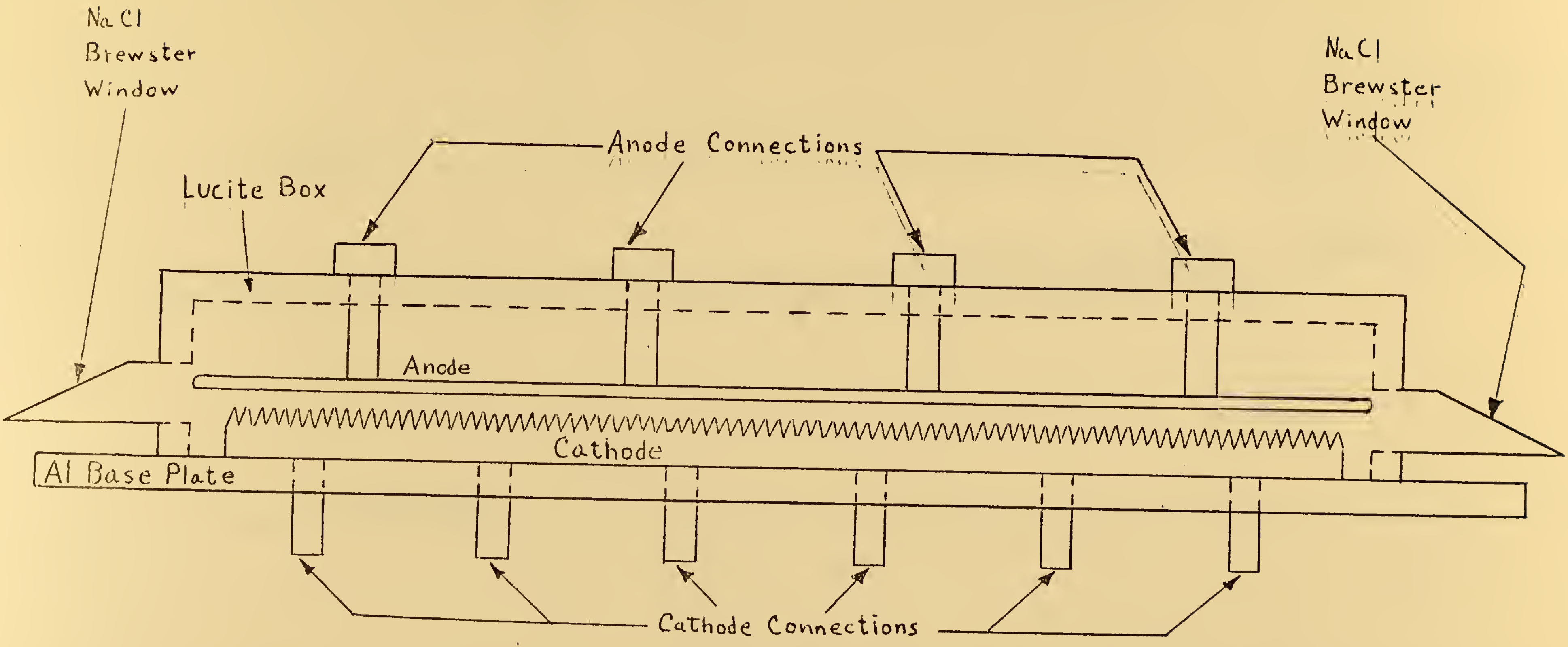

LASER CAVITY

(Scale: 1cm = 2inch)

Figure 9.

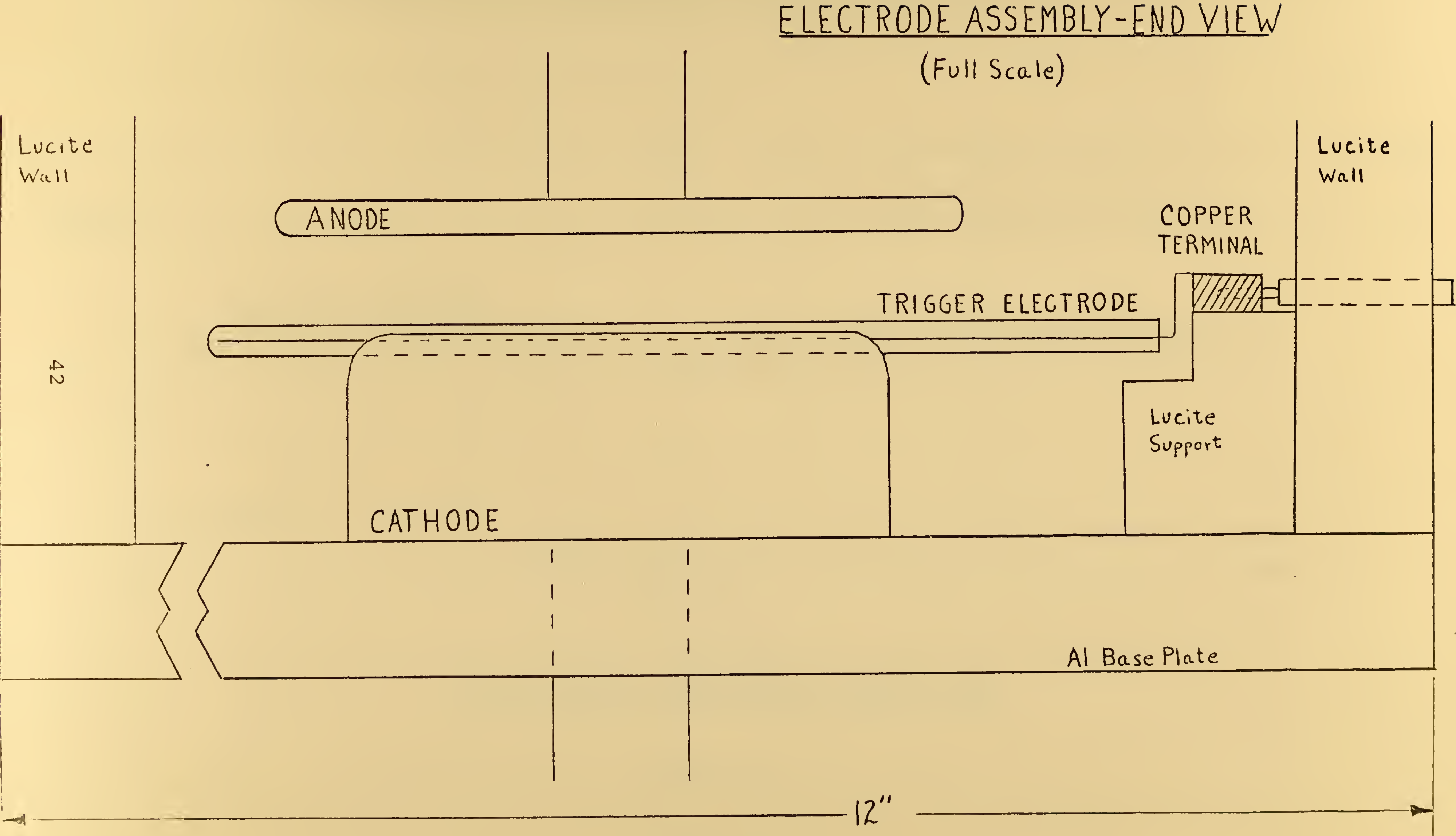
ELECTRODE ASSEMBLY-END VIEW
(Full Scale)
Lucite Wall
ANODE
COPPER TERMINAL
Lucite Wall
TRIGGER ELECTRODE
Lucite Support
CATHODE
Al Base Plate
12"

Figure 10.

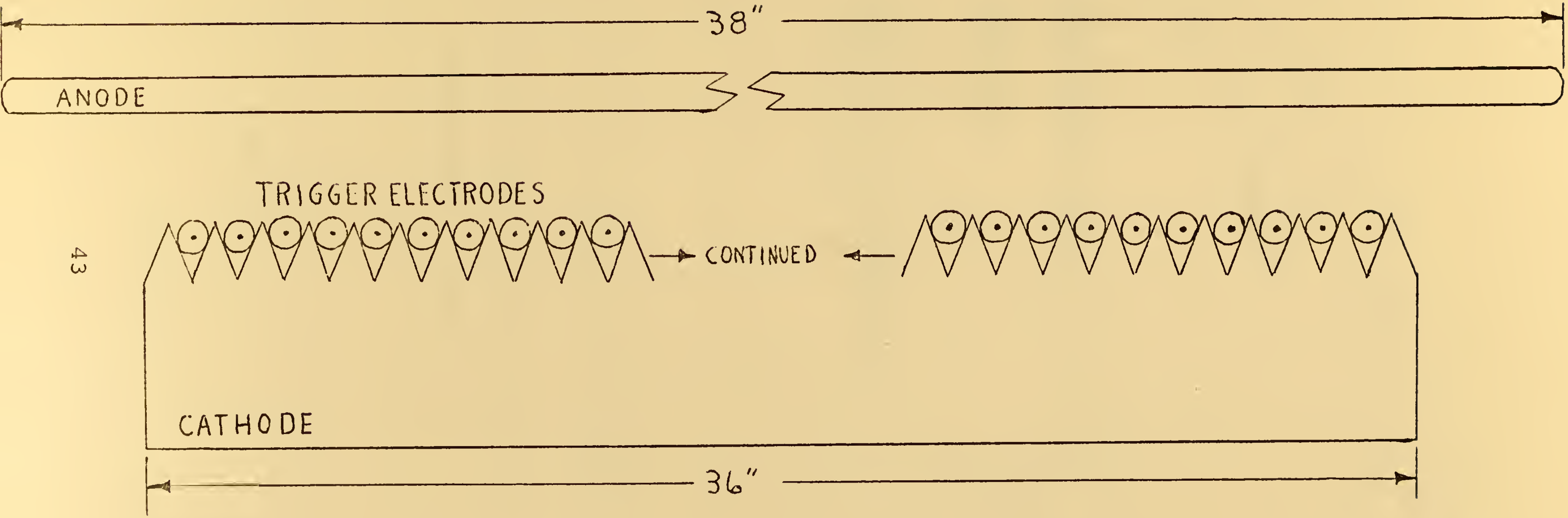

ELECTRODE ASSEMBLY- SIDE VIEW

Figure 11.

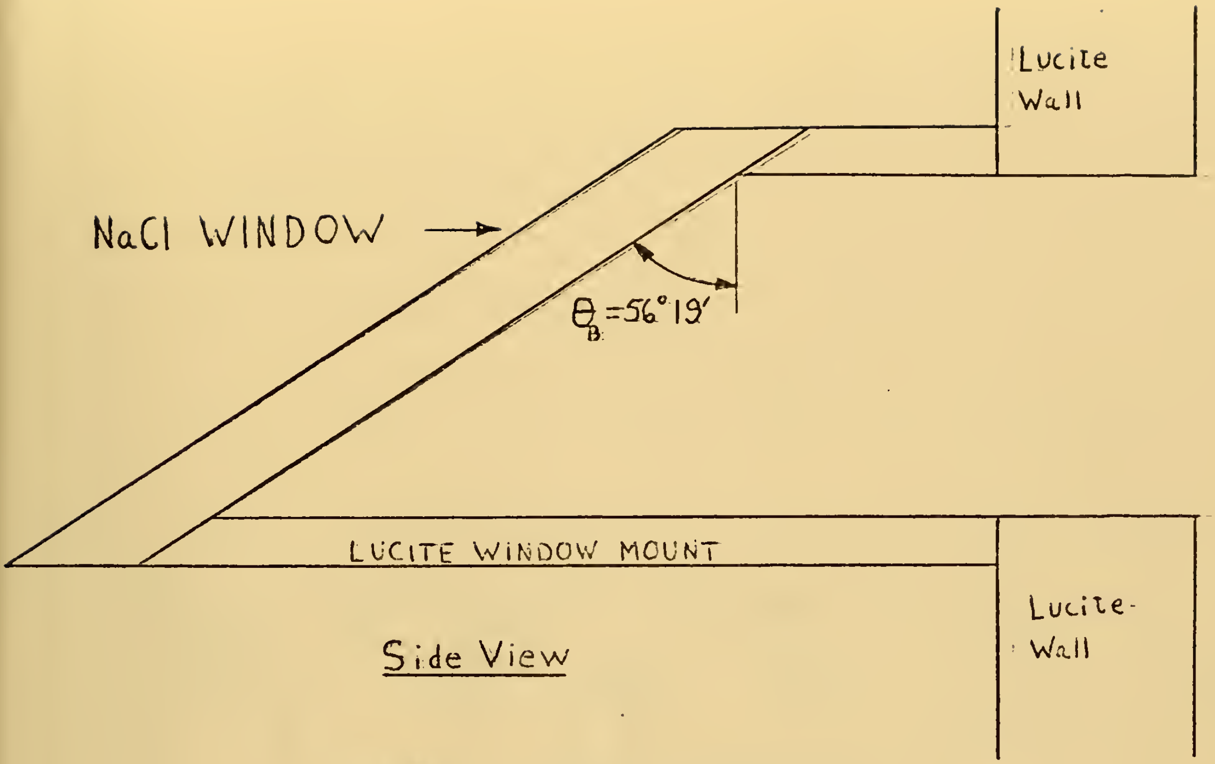

Side View

BREWSTER WINDOWS
(Full Scale)

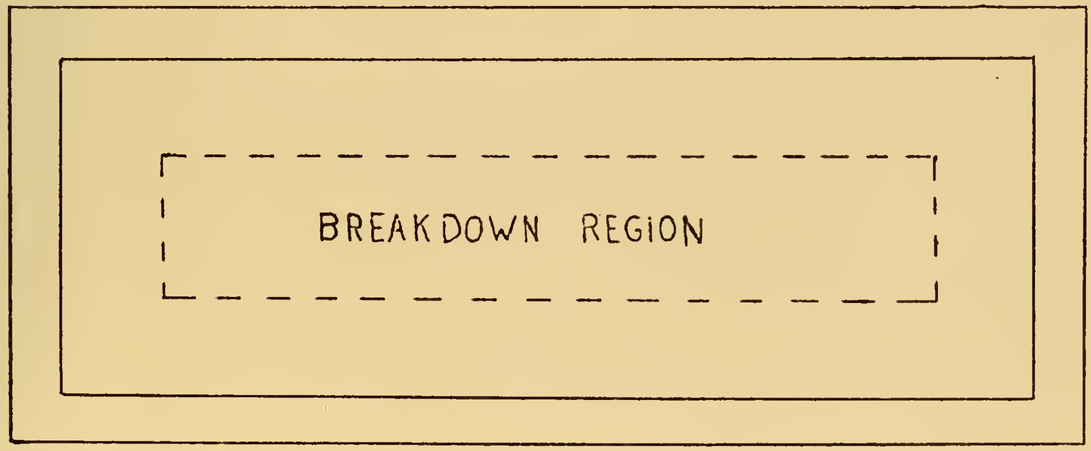

End View

Figure 12.

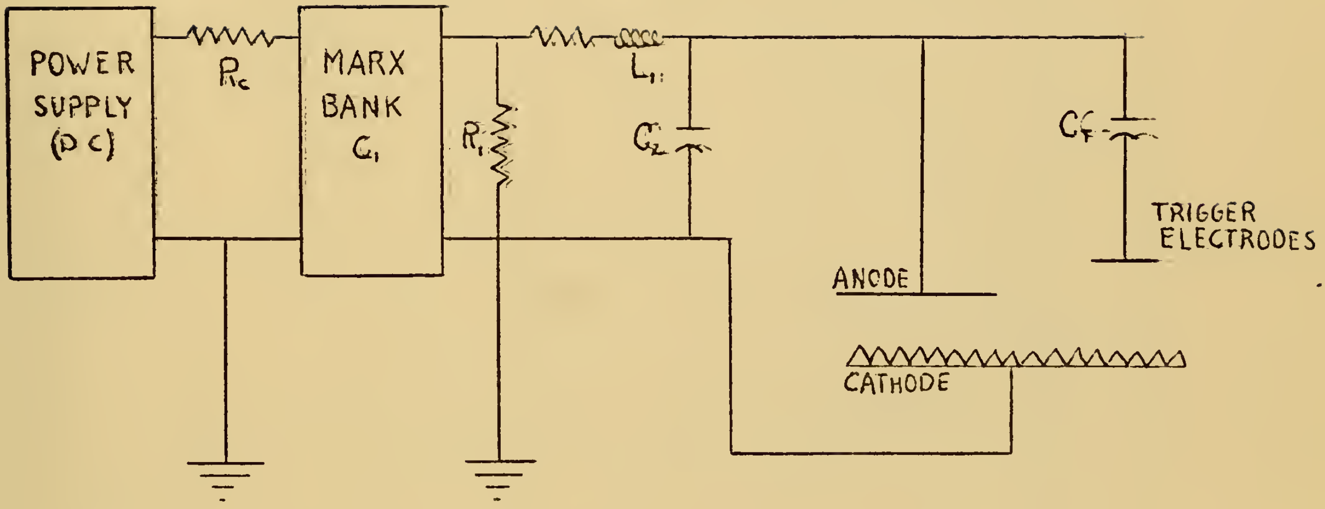

ELECTRICAL CIRCUIT

Figure 13.

OUTPUT MIRROR -(Full Scale)

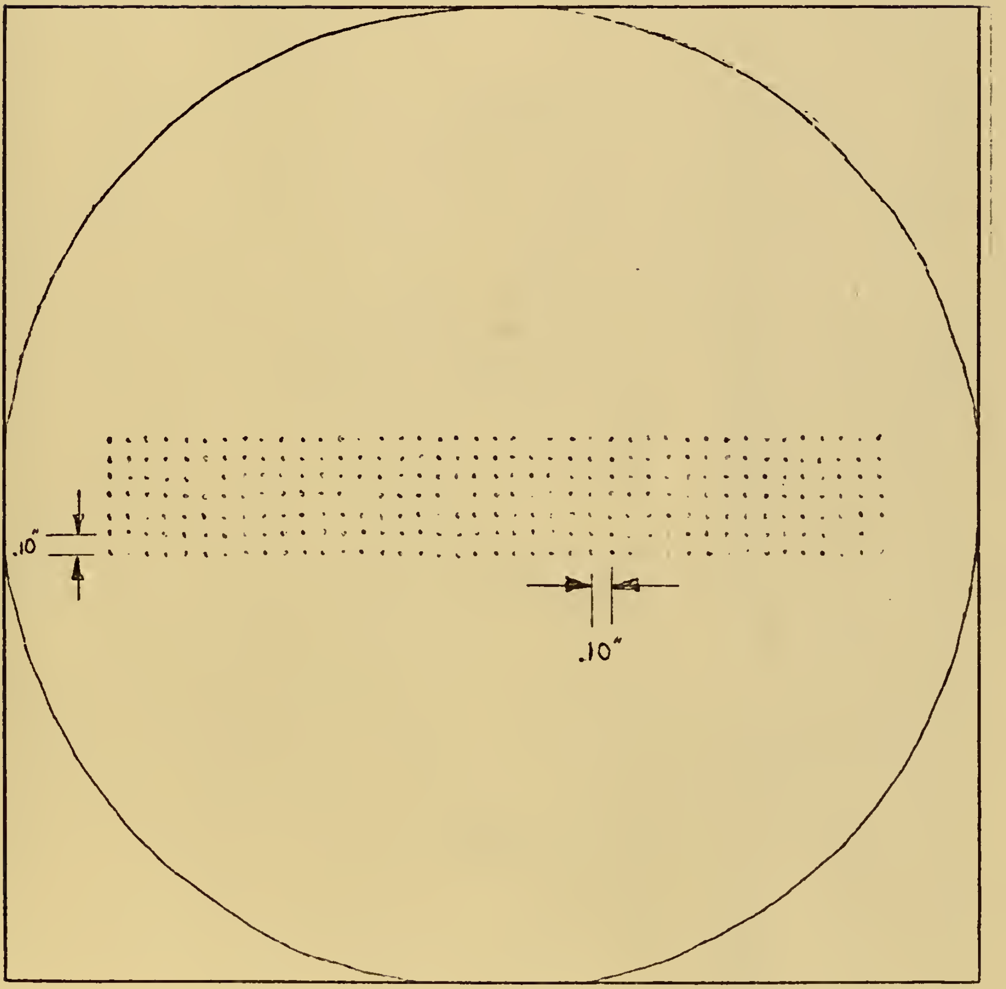

Hole Diameter = 0.334 mm
Radius of Curvature = 1 meter

Figure 14

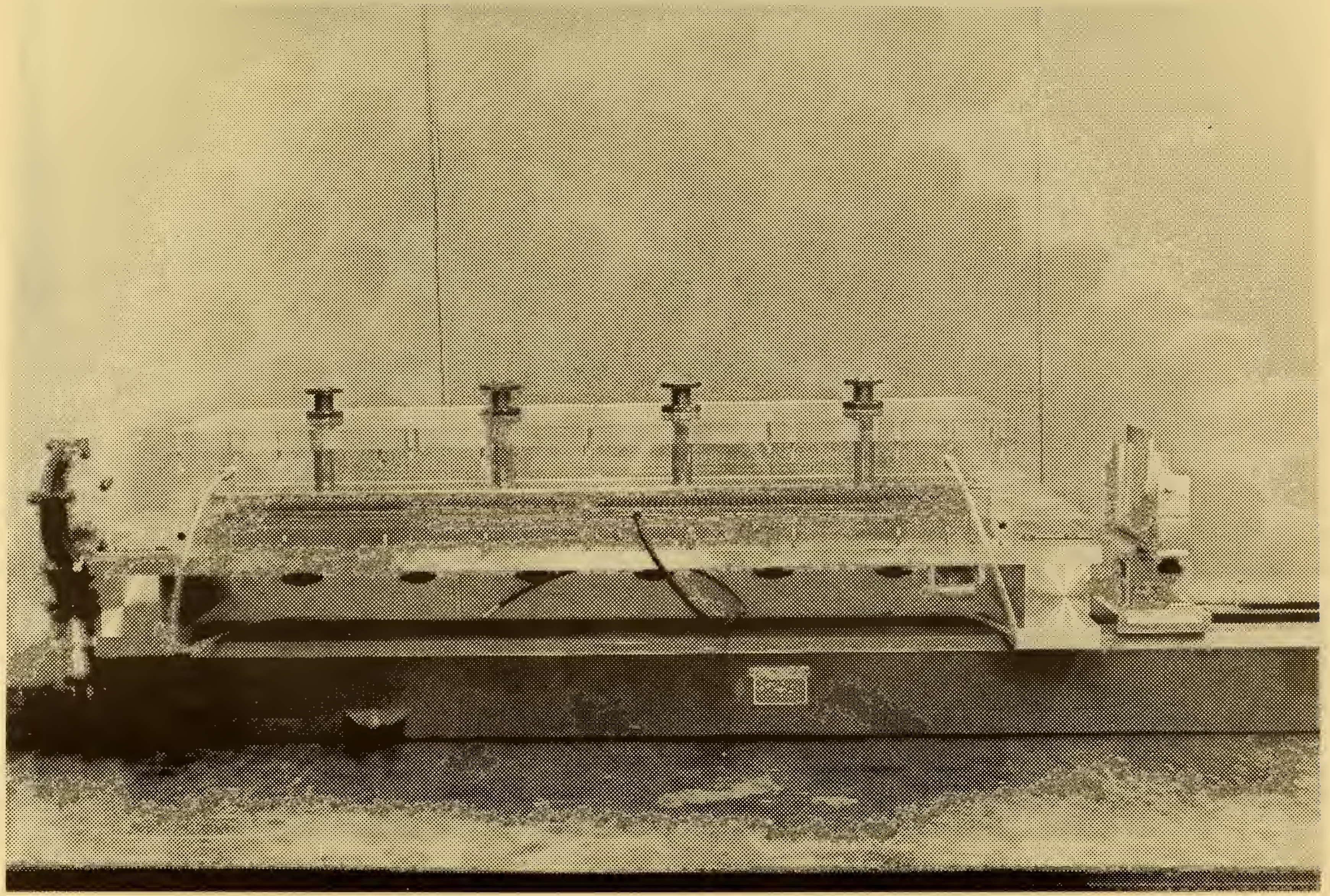

(1) LASER CAVITY

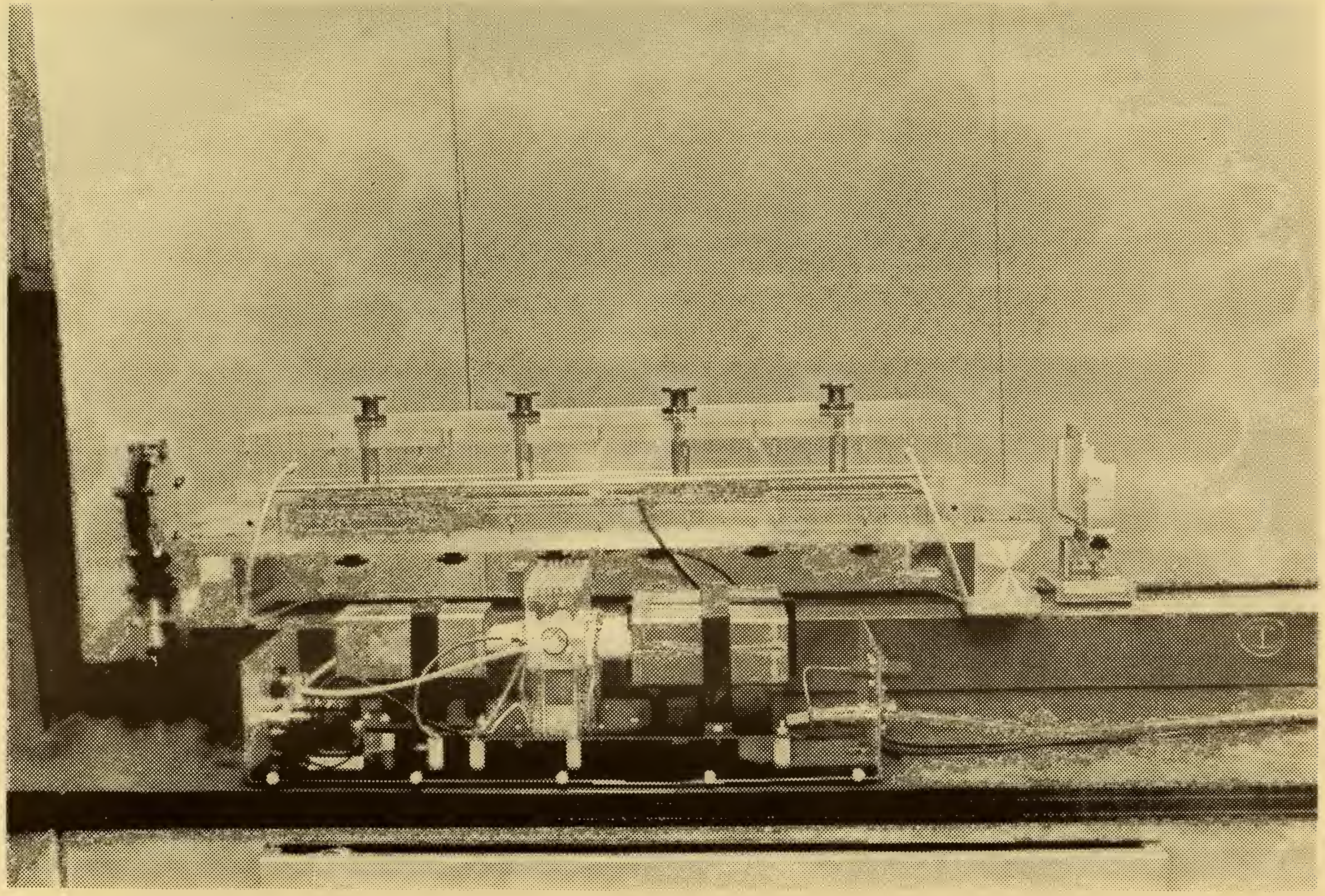

(2) MARX GENERATOR WITH LASER CAVITY

[illegible]

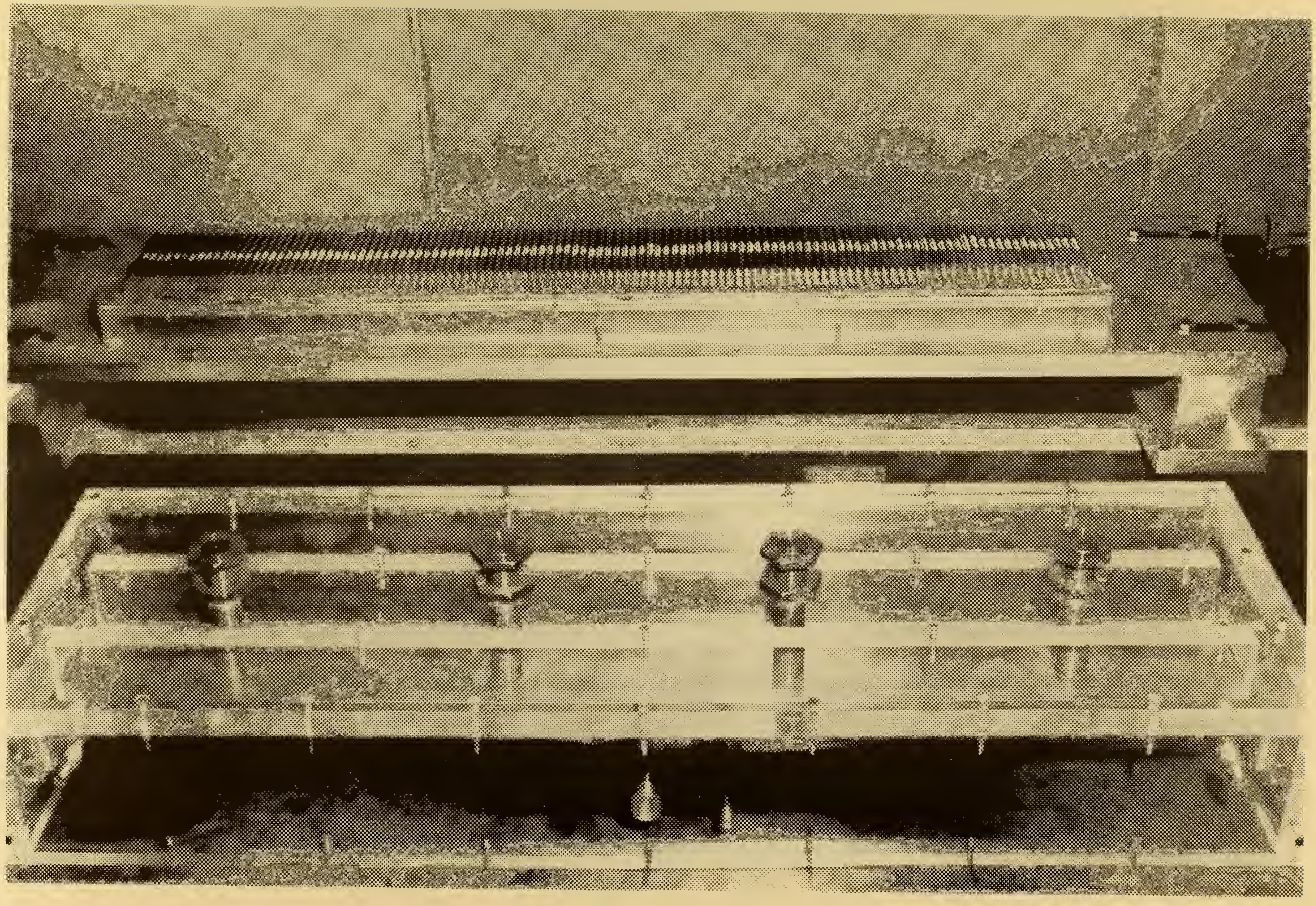

(3) CATHODE AND TRIGGER ASSEMBLY

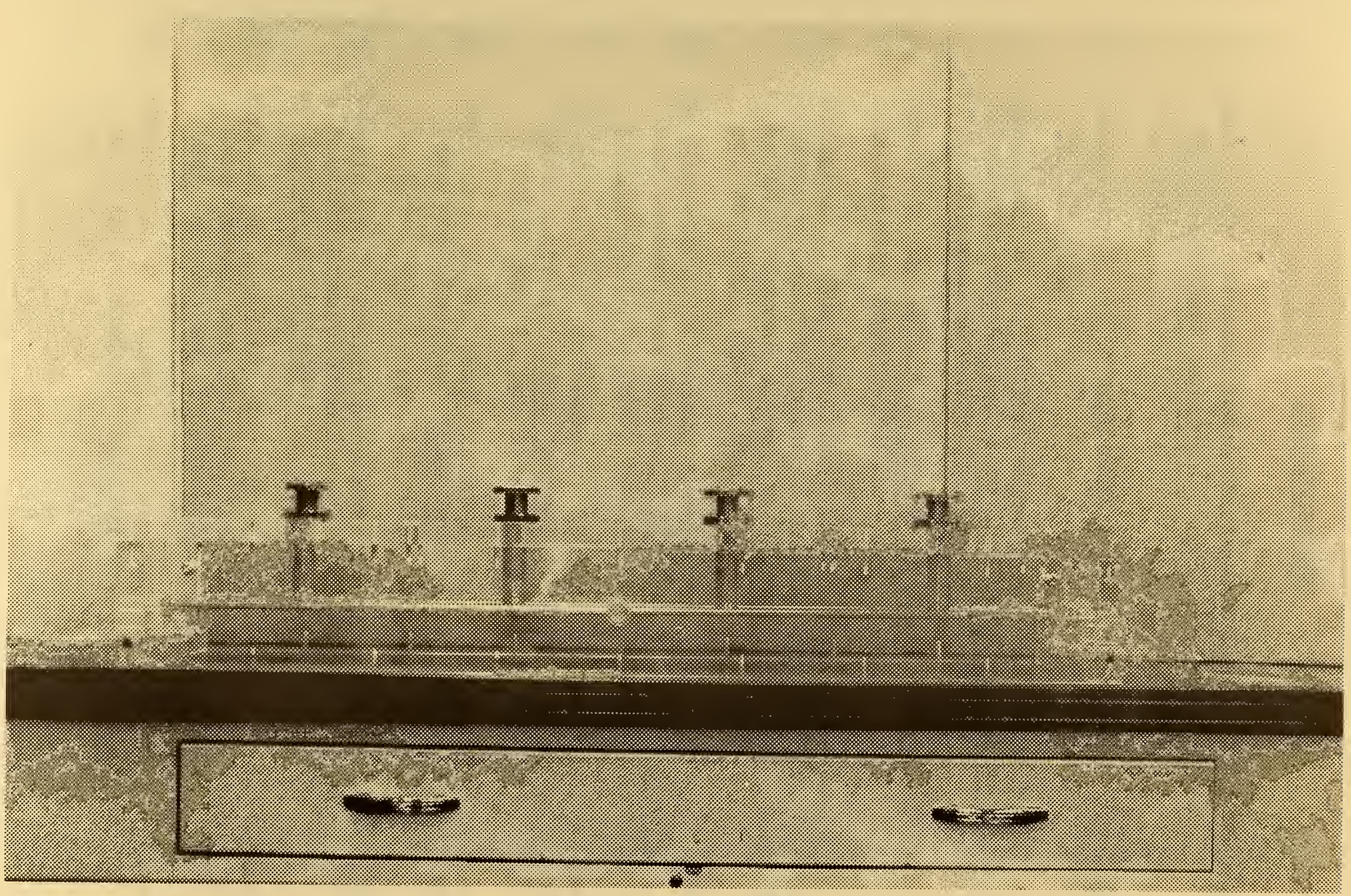

(4) LUCITE BOX WITH ANODE

BIBLIOGRAPHY

1. Aerospace Research Laboratories, *Reliable Spark Gap for Capacitor Bank Switching*, by W. D. Bunting, Jr., November 1963.

2. Beaulieu, A. J., "High Peak Power Gas Lasers," *Proceedings of the IEEE*, v. 59, no. 4, pp. 667-674, April 1971.

3. Beaulieu, A. J., "Transversely Excited Atmospheric Pressure CO_2 Lasers," *Applied Physics Letters*, v. 16, no. 12, pp. 504-505, 15 June 1970.

4. Bowen, E. G., ed, *A Textbook of Radar*, pp. 85-86, The University Press, 1954.

5. Bridges, T. J., and Chang, T. Y., "Pulse Response of Electro Optic Modulators and Photoconductive Detectors at 10.6 Microns, "*Applied Physics Letters*, v. 12, No. 9, pp. 297-300, 1 May 1968.

6. De Michelis, C., "Laser Interaction with Solids - A Bibliographical Review," *IEEE Journal of Quantum Electronics*, v. QE-6, No. 10, pp. 630-646, October 1970.

7. Dumanchin, R., and others, "Extension of TEA CO_2 Laser Capabilities," *IEEE Journal of Quantum Electronics*, v. QE-8, No. 2, pp. 163-165, February 1972.

8. Freiberg, R. J., and Clark, P. O., "CO_2 Transverse - Discharge Lasers," *IEEE Journal of Quantum Electronics*, V. QE-6, No. 2, pp. 105-113, February 1970.

9. Fortin, R., "Preliminary Measurements of a Transversely Excited Atmospheric Pressure CO_2 Laser," *Canadian Journal of Physics*, V. 49, pp. 257-264, 1971

10. Fox, A. G., and Li, T., "Modes in a Maser Interferometer with Curved and Tilted Mirrors," *Proceedings of the IEEE*, V. 51, No. 1, pp. 80-89, January 1963.

11. Gibson, A. F., Kimmit, M. F., and Walker, A. G., "Photon Drag in Germanium," *Applied Physics Letters*, V. 17, No. 2, pp. 75-77, 15 July 1970.

12. Knoepfel, H. E., *Pulsed High Magnetic Fields*, pp. 143-145, American Elsevier, 1970.

13. Laurie, K. A., and Hale, M. M., "Folded-Path Atmospheric Pressure CO_2 Laser," *IEEE Journal of Quantum Electronics*, pp. 530-532, August 1970.

14. Los Alamos Scientific Laboratory, *Considerations in the Design of Energy Storage Capacitor Banks*, by Kemp, E. L., 20 June 1961.

15. McNice, G. T., and Derr, V. E., "Analysis of the Cylindrical Confocal Laser Resonator Having a Single Circular Coupling Aperture," *IEEE Journal of Quantum Electronics*, V. QE-5, No. 12, pp. 569-575, December 1969.

16. Pan, Y. L., Bernhardt, A. A., and Simpson, J. R., *On the Construction and Operation of a Double-Discharge TEA CO_2 Laser*, Lawrence Radiation Laboratories paper submitted to the Review of Scientific Instruments, 22 September 1971.

17. Patel, C. K. N., "High Power Dioxide Lasers," *Scientific American*, pp. 265-275, August 1968.

18. Patel, C. K. N., and others, "Laser Action Up to 57.355 Microns in Gaseous Discharges," *Applied Physics Letters*, v. 4, No. 1, pp. 18-19, 1 January 1964.

19. Pearson, P. R., and Lamberton, H. M., "Atmospheric Pressure CO_2 Lasers Giving High Output Energy Per Unit Pulse," *IEEE Journal of Quantum Electronics*, V. QE-8, no. 2, pp. 145-149, February 1972.

20. Siegman, A. E., *An Introduction to Lasers and Masers*, McGraw-Hill, 1971.

21. Sinclair, D. C., *Gas Laser Technology*, Holt Rinehardt, 1969.

22. Smith, D. C., and Berger, P. J., "Mode-Locking of an Atmospheric Pressure Cross Excited Electrically Pulsed CO_2 Laser," *IEEE Journal of Quantum Electronics*, pp. 173-174, April 1971.

23. Smith, D. C., and De Maria, A. J., "Parametric Behavior of the Atmospheric Pressure Pulsed CO_2 Laser," *Journal of Applied Physics*, v. 41, No. 13, pp. 5212-5214, December 1970.

24. Sohoo, R. F., "Nonconfocal Multimode Resonators for Masers," Proceedings of the IEEE, V. 51, No. 1, pp. 70-75, January 1963.

25. Tachisto, Inc., "Instruction Manual for Series MC3 Impulse Generators," March 1972.

26. Willett, C. S., and Gleason, T. J., "Gas Lasers at Room Pressure," Laser Focus, pp. 30-34, June 1971.

INITIAL DISTRIBUTION LIST

		No. Copies
1.	Defense Documentation Center Cameron Station Alexandria, Virginia 22314	2
2.	Library, Code 0212 Naval Postgraduate School Monterey, California 93940	2
3.	Assoc Professor Fred R. Schwirzke Department of Physics Naval Postgraduate School Monterey, California 93940	3
4.	Asst Professor Natale M. Ceglio Department of Physics Naval Postgraduate School Monterey, California 93940	1
5.	LT Ronald F. Bishop SMC 1853 Naval Postgraduate School Monterey, California 93940	1
6.	Captain Douglas H. Barr, USA Staff and Faculty ADA School Ft. Bliss, Texas 79906	1

DOCUMENT CONTROL DATA - R & D

(Security classification of title, body of abstract and indexing annotation must be entered when the overall report is classified)

1. ORIGINATING ACTIVITY *(Corporate author)* Naval Postgraduate School Monterey, California 93940	2a. REPORT SECURITY CLASSIFICATION Unclassified 2b. GROUP

3. REPORT TITLE

Construction of a Carbon Dioxide TEA Laser

4. DESCRIPTIVE NOTES *(Type of report and inclusive dates)*

Master's Thesis; June 1972

5. AUTHOR(S) *(First name, middle initial, last name)*

Douglas Harmon Barr

6. REPORT DATE June 1972	7a. TOTAL NO. OF PAGES 56	7b. NO. OF REFS 26

8a. CONTRACT OR GRANT NO.	9a. ORIGINATOR'S REPORT NUMBER(S)
b. PROJECT NO.	
c.	9b. OTHER REPORT NO(S) *(Any other numbers that may be assigned this report)*
d.	

10. DISTRIBUTION STATEMENT

Approved for public release; distribution unlimited.

11. SUPPLEMENTARY NOTES	12. SPONSORING MILITARY ACTIVITY Naval Postgraduate School Monterey, California 93940

13. ABSTRACT

The recent development of CO_2 Transverse Excitation at Atmospheric Pressure (TEA) lasers has generated expanding interest and success due to their high pulsed power capabilities and simplicity of construction. We therefore decided to construct a CO_2 TEA laser because of the need for a high powered, pulsed, coherent radiation source with wave length near 10 microns to conduct absorption studies of laser-induced plasmas. It was decided that the constructed laser should have an output energy per pulse between 10 to 50 joules with a pulse time between 0.1 to 1.0 microseconds. This paper deals with the construction of that laser, and includes a discussion of the background and physics of operation of the CO_2 TEA laser.

DD FORM 1 NOV 65 1473 (PAGE 1)

S/N 0101-807-6811

Unclassified

Security Classification

A-31408

KEY WORDS	LINK A		LINK B		LINK C	
	ROLE	WT	ROLE	WT	ROLE	WT
TEA Laser						
Carbon Dioxide Laser						
Transverse excitation						
Pulsed power						
Infrared Radiation						
Marx Generator						

17 JUN 74
7 SEP 76

21053
23738

Thesis
B235 Barr
c.1

134815

Construction of a carbon dioxide TEA laser.

4 JUN 74 21053
17 JUN 74 21053
7 SEP 76 23738

Thesis
B235 Barr
c.1

134815

Construction of a carbon dioxide TEA laser.

thesB235
Construction of a carbon dioxide TEA las
3 2768 002 01445 8
DUDLEY KNOX LIBRARY